

Determining the electronic triplet-singlet transition probability in double quantum dots: Analogy with the double slit experiment

Fernando Domínguez and Gloria Platero

Instituto de Ciencia de Materiales de Madrid, CSIC, Cantoblanco, Madrid 28049, Spain

We apply an elementary measurement scheme to calculate the electronic triplet-singlet transition mediated by hyperfine interaction in a double quantum dot. We show how the local character of the hyperfine interaction and the nuclear back-action process (flip-flop) are crucial to cancel destructive interferences of the triplet-singlet transition probability. It is precisely this cancellation which differentiates the hyperfine interaction from an anisotropic magnetic field which mixes the triplet and the singlet eigenstates.

PACS numbers:

Experimental progress during the last two decades has opened the possibility to reduce semiconductor devices to the nanometer scale, such as quantum wires and quantum dots. Furthermore, coherent control of electronic transport and spin manipulation in quantum dots¹ is also possible due to the long spin relaxation time². These two facts lead us to think of quantum dots as the minimal structures of computers based on quantum mechanical principles, i.e., quantum computers. Quantum properties such as entanglement or quantum parallelism will be used as algorithm tools³. However, there are still a lot of obstacles that separate us from the construction of such a computer. A major source one comes from decoherence through the interaction with the environment. Special attention has been paid to the interaction between the nuclear and the electronic spins by means of the hyperfine interaction (HF)^{4,5,6}. The importance of this well-known decoherence process is clearly manifest in a very known system: a double quantum dot (DQD) in the spin blockade regime (SB)^{7,8,9,10,11,12,13}. There, the occupation depends on the spin degree of freedom and sequential transport is blocked due to the Pauli exclusion principle. In this way, whenever the transport is blocked, a current may arise only when spin scattering processes such as HF interaction flips one of the electronic spins^{7,8}, inducing the triplet-singlet transition ($T_{\pm 1}-S$).

Many experiments have been performed in a lateral DQD in the SB regime. Some of them show a hysteretic behavior upon sweeping the magnetic field^{10,11}. Besides this hysteretic behavior, other experiments in the strong interdot coupling regime show how current changes radically and prominent current spikes appear tuning the in-plane magnetic field¹¹. Motivated by these recent experiments, we have studied microscopically the $T_{\pm 1}-S$ transition probability induced by the HF interaction in a lateral DQD. The $T_{\pm 1}-S$ transition determines transport and serves as a basis to study the nuclear dynamical polarization, providing the possibility to study quantitatively the current in any interdot coupling regime.

Double slit analogy.—Before starting to calculate the transition rate, let us discuss some physical aspects which make the HF interaction different from other interactions such as the spin-orbit interaction or an anisotropic mag-

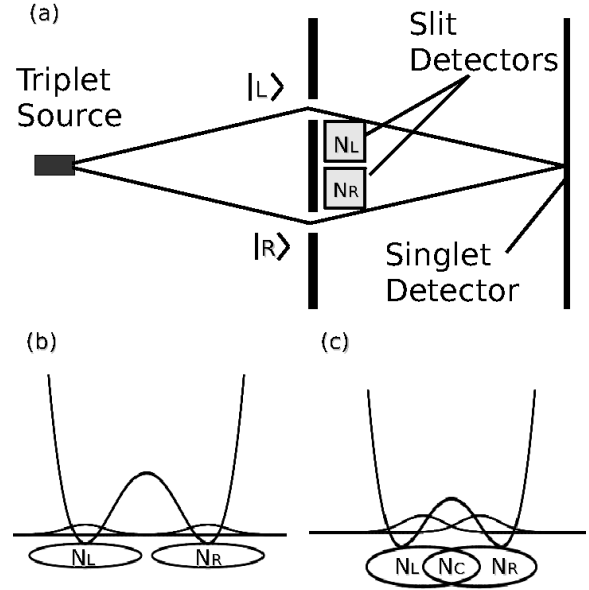


FIG. 1: (a) Spin Blockade regime shown in the scheme of the double slit experiment. Schematic drawn of the atomic envelope functions of a DQD in the (b) weak, (c) strong coupling regimes.

netic field. The HF interaction has two special characteristics: the first one is its local character. Thus, the electronic envelope function determines the number of nuclei which can interact with the electronic spin. Therefore, it is natural to associate an ensemble of nuclear spins to each quantum dot (N_L and N_R in Figs. 1b and c). The second one is related to spin conservation. Whenever there is an electronic spin-flip transition ($T_{\pm 1}-S$), the spin orientation of one nuclear spin localized in one of the two baths, N_L or N_R , is reversed. It is precisely this local change which allows one to detect in which of the dots the electronic spin flips. In analogy to the double slit experiment, we will show that the negative $T_{\pm 1}-S$ interference pattern is completely destroyed when the nuclear spin ensembles measure exactly in which of the dots is the spin-flip produced (Fig. 1b). To complete

our analysis, we have considered the case where some of the nuclear spins interact with both dots (Fig. 1c), which occurs when the electronic wave function is extended, i.e., strong interdot coupling. As we will see, the shared bath give rise to an uncertainty in the local measurement of the spin-flip, leading to the appearance of negative interference terms proportional to the overlap of the electronic wave functions.

Considering the nuclear spin bath as a slit detector is supported by the fact that nuclear spins have no internal dynamics¹⁴. Estimations of nuclear spin dynamics, due to dipole-dipole nuclear spin interaction, suggest that time scales governing nuclear spin evolution ($t > 100\text{ms}$) are orders of magnitude slower than other associated with electron spin processes⁵. Thus, we consider only changes of the nuclear spin states induced by the HF interaction with the electrons. If the internal nuclear spin dynamics were not frozen, one would take them into account⁶.

Transition rate.—In our model, the eigenstates of two electrons trapped in a lateral DQD are obtained by using the Heitler-London approximation. This approximation has been widely used in the DQD context¹⁵. The electronic wave functions are described by the direct product of spin and orbital wave functions. The spin state is given by the known singlet-triplet basis, while the orbital part is composed by the displaced Fock-Darwin states $\langle \mathbf{r}|L\rangle$ and $\langle \mathbf{r}|R\rangle$, which are the exact atomic states

$$|\phi_{\pm}\rangle = \frac{|L(1)R(2)\rangle \pm |L(2)R(1)\rangle}{\sqrt{2(1 \mp O^2)}}, \quad (1)$$

with $O = \int d^2r \langle L|\mathbf{r}\rangle \langle \mathbf{r}|R\rangle$ corresponding to the overlap of the right and left orbitals. The sign $+(-)$ corresponds to the singlet (triplet) state, while the numbers 1 and 2 label the electrons. In the spin blockade regime, electrons are found in the triplet states $|T_{\pm 1}\rangle$, where the two electrons have parallel spin polarization.

The hyperfine interaction can be seen as the scattering between electronic and the nuclear spin wave functions. The above mentioned characteristics expressed by the contact Hamiltonian¹⁶

$$V_{HF} = \frac{A}{N_L} \sum_{k=1}^{N_L} \sum_{i=1,2} (S_i^+ I_{L,k}^- + S_i^- I_{L,k}^+ + S_i^z I_{L,k}^z) + \frac{B}{N_R} \sum_{k=1}^{N_R} \sum_{i=1,2} (S_i^+ I_{R,k}^- + S_i^- I_{R,k}^+ + S_i^z I_{R,k}^z), \quad (2)$$

where S_i^{\pm} are the raising/lowering spin operators of the electron i . The $I_{L(R),k}^{\pm}$ are the raising/lowering of the k th

nuclear spin operator. The subscripts L and R denote in which of the dots are placed the nuclear spins. $N_{L(R)}$ is the number of nuclear spins which interact with an electron when it is localized in the left (right) dot. A and B are the hyperfine interaction constants for the left and the right dot, respectively.

Terms containing the raising and the lowering operators describe the dynamic part of the hyperfine interaction, they are responsible for the electronic-nuclear spin-flip. On the other hand, the z -projection terms give rise to an additional Zeeman splitting, called Overhauser shift.

Having defined the DQD eigenbasis and the HF Hamiltonian, we are ready to study the decoherence produced by the spin environment in the $T_{\pm 1}$ - S transition. In order to describe completely the $T_{\pm 1}$ - S transition, we must include the nuclear states in the initial and final wave functions¹⁴. Thus, we obtain the transition probability rate

$$\begin{aligned} \mathcal{P}_{T \rightarrow S} &= \sum_{k=1}^N |\langle m_{f,k} | \langle S | V_{HF} | T_{\pm 1} \rangle | m_i \rangle|^2 \\ &= \sum_{k=1}^N \langle S | \langle m_{f,k} | \rho | m_{f,k} \rangle | S \rangle, \end{aligned} \quad (3)$$

where $\rho = V_{HF} | T_{\pm 1} \rangle | m_i \rangle \langle m_i | \langle T_{\pm 1} | V_{HF}$. We have defined N as the total number of nuclear spins which interact in the dots. The initial nuclear spin state

$$|m_i\rangle = \prod_{k=1}^N |\sigma_k\rangle, \quad (4)$$

is an eigenstate of I_z . Here σ_k is the z -component of the k th nuclear spin. The states $|m_{f,k}\rangle$ for k from 1 to N , represent all possible final nuclear spin states. Depending on the electronic initial state $|T_{\pm 1}\rangle$, it is defined as $|m_{f,k}\rangle = I_k^{\pm} |m_i\rangle$ where I_k^{\pm} are the raising/lowering k th nuclear spin operators. $|m_{f,k}\rangle$ is zero in the case where the initial k th nuclear spin is parallel oriented with respect to the electronic spins $|T_{\pm 1}\rangle$. In order to make the discussion clearer, we restrict the calculation to the initial electronic state $|T_{+1}\rangle$. Notice that in this case the contribution to the T_{+1} - S transition comes from the down oriented nuclear spins.

The HF interaction entangles the electronic and the nuclear wave functions. Operating the initial state $|\Psi\rangle = |T_{+1}\rangle |m_i\rangle$ by means of the HF Hamiltonian (2), we obtain

$$V_{HF}|\Psi\rangle = \frac{1}{\sqrt{2(1+O^2)}} \left[|\uparrow_1, \downarrow_2\rangle \left(\frac{B}{N_R} |L(1)R(2)\rangle |M_R\rangle - \frac{A}{N_L} |L(2)R(1)\rangle |M_L\rangle \right) + |\downarrow_1, \uparrow_2\rangle \left(\frac{A}{N_L} |L(1)R(2)\rangle |M_L\rangle - \frac{B}{N_R} |L(2)R(1)\rangle |M_R\rangle \right) \right], \quad (5)$$

where

$$|M_{L(R)}\rangle \equiv \sum_{k=1}^{N_{L(R)}} I_{L(R),k}^+ |m_i\rangle, \quad (6)$$

is a linear combination of nuclear states, where one of the nuclear states of the $L(R)$ dot has been flipped from \downarrow to \uparrow , i.e. $N_{R(L),\downarrow}$. Each component of the sum (6) belongs to the final state basis $\{|m_{f,k}\rangle\}$. $|M_{L(R)}\rangle$ contains as many terms as nuclear spins \downarrow interact with an electron localized in the dot $L(R)$.

Using eq. (5) we can calculate directly the product $\rho = V_{HF}|\Psi\rangle\langle\Psi|V_{HF}$. Finally we have to carry out the projection on the final nuclear (nuclear trace out) and electronic (singlet) states. Before presenting the general results, it is convenient to evaluate first scalar products involved in the nuclear trace

$$\sum_{k=1}^N \langle m_{f,k} | M_i \rangle \langle M_j | m_{f,k} \rangle = \langle M_i | M_j \rangle, \quad (7)$$

for i and j equal to L and R . First of all, we evaluate the case $i = j$. Due to orthogonality, the projection of each component of state (6) contributes to the total scalar product with unity, if two equal components are projected, and zero otherwise. With this in mind it is easy to calculate

$$\langle M_{L(R)} | M_{L(R)} \rangle = N_{L(R),\downarrow}. \quad (8)$$

On the other hand, the meaning of the scalar product with $i \neq j$ is more subtle. If we had imagined $|M_L\rangle$ and $|M_R\rangle$ as two independent spaces, we would say that no term survives due to orthogonality conditions. In principle, this argument looks to be reasonable, but care must be taken due to the existence of an overlap between the atomic wave functions O^2 . The existence of such an overlap implies that both electrons can interact with a common ensemble of nuclear spins at the same time, see Fig. 1(c). Mathematically this is reflected by the fact that $|M_L\rangle$ and $|M_R\rangle$ contain a common nuclei ensemble

$$\langle M_L | M_R \rangle = N_{C,\downarrow}, \quad (9)$$

where $N_{C,\downarrow}$ is the number of nuclei that can be flipped by both electrons placed in different dots. Obviously this number is proportional to the overlap. It must be noted that $N_{i,\downarrow}$ refers to those nuclei that can interact only with the electron localized at dot i and others which can

interact with both of them. Thinking in terms of detectors, we would say that the existence of the shared bath gives rise to an uncertainty in the localization of the electronic spin-flip. Thus, the higher $N_{C,\downarrow}$, the less reliable the spin-flip detectors and the more pronounced the negative interference pattern.

Finally, we replace the obtained expressions (5), (8), (9) into (3), yielding

$$\mathcal{P}_{T \rightarrow S} = D \left(B^2 \frac{N_{R,\downarrow}}{N_R^2} + A^2 \frac{N_{L,\downarrow}}{N_L^2} - 2AB \frac{N_{C,\downarrow}}{N_L N_R} \right), \quad (10)$$

where we have used $D = (1 + O^2) / (1 - O^2)$. Equation (10) is the main result of our work. It is composed by three terms, the first two arise due to the contribution of the nuclear spins of each dot which are able to flip the electronic spin, while the third one arises due to the uncertainty in the measurement of the spin-flip position ($N_{C,\downarrow}$), caused by the overlap of the electronic wave functions. We observe a change the tunnel interdot on the interference pattern. In the weak-coupling regime, the interference tends to zero since the overlap is negligible ($O^2 \rightarrow 0$). In this case, nuclear detectors are perfectly reliable and thus the interference term of eq. (10) is cancelled⁸. On the other hand, in the strong-coupling regime the overlap is not negligible and an uncertainty in the spin-flip position arises and leads to the appearance of a negative interference pattern. It must be noted the fundamental difference between the HF interaction and the effect of an inhomogeneous magnetic field, in the case of the inhomogeneous magnetic field the interference pattern holds, leading to a probability which depends on the difference between the in-plane effective magnetic fields of each dot¹².

Let us extend our analysis to the transition rates between the triplet states $T_{\pm 1}$ and T_0 . It yields a similar expression as (10), except for D which becomes one, and the negative sign of the interference pattern which becomes positive. On the other hand, the states T_0 and S are mixed due to the difference between the Zeeman splittings within each dot, i.e., due to the magnetic field anisotropy¹⁸.

Current—In order to show how the obtained transition rate (10) determines a measurable quantity as the current, we analyze transport in the strong interdot coupling regime by means of a simple model. We focus on the following transport configuration: zero detuning, low in-plane magnetic field and strong interdot coupling, we consider the schematic picture of the different spin-flip transitions depicted in Fig. 2¹¹. At this experimental

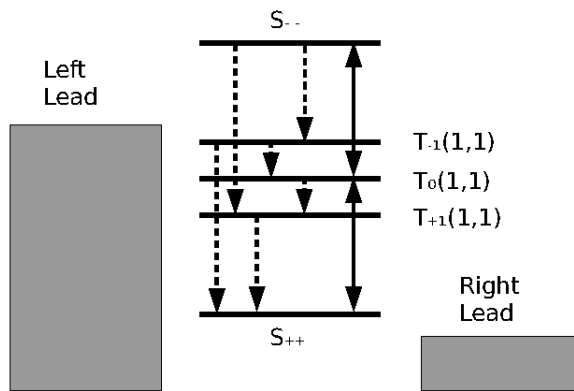


FIG. 2: Transport window scheme of a DQD in the sharp transport regime. The dashed arrows represent spin-flip phonon assisted transitions, while the double arrows represent coherent couplings due to the inhomogeneous Overhauser field.

conditions, the energy difference between the $T(1,1)$ and $S(1,1)$ (T_0 and $T_{\pm 1}$) states is larger than the nuclear Zeeman splitting. Therefore, at low temperatures only transitions $T_{\pm 1}-S$ and $T_{\pm 1}-T_0$ involving phonon emission are efficient¹⁹.

We calculate the stationary current through the DQD based in a model presented in reference¹². Within a density matrix formalism, considering the electron reservoirs within Markov approximation. The system involves seven diagonal matrix elements: three triplet states $T(1,1)$, two singlet states $S_{++} = \frac{1}{\sqrt{2}}(S(1,1) + S(0,2))$ and $S_{--} = \frac{1}{\sqrt{2}}(S(1,1) - S(0,2))$ and two single occupied states¹⁷. Additionally, it involves six non-diagonal matrix elements, corresponding to the coherences between the singlet states S_{++} , S_{--} and the triplet $T_0(1,1)$ states, which are mixed by the anisotropy of the Overhauser field (ΔB_z). We calculate the stationary current making the time derivatives equal to zero. Aiming at simplicity, the triplet states $T(1,1)$ and the extended singlet state S_{++} are coupled to the left lead while S_{++} and S_{--} are coupled to the right, by means of the coupling constant Γ . The current is proportional to the occupation of

the state $S(0,2)$ and can be calculated analytically for the general case. The general solution is quite lengthy but it can be simplified assuming that $\Delta B_z \ll E_S - E_T$ and that the transition rate Γ is orders of magnitude higher than the spin-flip rates, yielding

$$I = \frac{7\beta\delta(\alpha + \delta)}{6\beta\delta + 2\delta(3\delta + 2\alpha) + 2\alpha\beta}, \quad (11)$$

where α and β represent the inelastic transition rates $T_{\pm 1}-S$, while δ represents the rates $T_{\pm 1}-T_0$. Obviously this simple model does not attempt to explain quantitative experimental evidences¹¹, but it is illustrative in order to show how the current is governed mainly by the transition rates $T_{\pm 1}-S$ and $T_{\pm 1}-T_0$ (10). To obtain a more detailed model one has to study the time evolution accounting for the dynamical polarization of the nuclear spin ensembles, which is responsible for current bistability among other non-linear effects⁸.

Conclusions.—We have presented a microscopic model to describe the triplet-singlet and triplet-triplet transition probabilities mediated by the HF interaction in a DQD. We have stressed the importance of the local character and the nuclear flip-flop process of the HF interaction. These characteristics lead to a partial cancellation of the interference pattern, which can be intuitively seen by means of an analogy between the triplet-singlet transition and the double-slit experiment. With this picture in mind, we have shown the fundamental difference between the transition mediated by the hyperfine interaction and an anisotropic magnetic field. The transition under study turned out to be relevant in the spin blockade regime. The obtained results will serve as a basis to study transport accounting for the nuclear spin dynamical polarization and will open the possibility to explain experiments covering different tunneling coupling regimes.

We like to thank C. López-Monís and J. Iñarrea for fruitful discussions and S. Kohler for helpful comments on the paper. This work has been supported by the Spanish project MAT2008-02626. F. D. acknowledges MEC (Spain) for financial support through the FPI predoctoral grant.

¹ R. Hanson *et al.*, Rev. Mod. Phys. **79**, 1217 (2007).

² T. Fujisawa, D. G. Austing, Y. Tokura, Nature 419, 278 (2002); A. C. Johnson *et al.*, Nature 435, 925 (2005).

³ A. Ekert and R. Josza, Rev. Mod. Phys. **68**, 733, (1996); C. H. Bennett and D. P. DiVicenzo, Nature (London) **404**, 247 (2000).

⁴ A. Khaetskii, D. Loss and L. Glazman, Phys. Rev. B, **67**, 195329 (2003).

⁵ I. A. Merkulov, A. Efros and M. Rosen, Phys. Rev. B **65**, 205309, (2002).

⁶ W. A. Coish *et al.*, J. Appl. Phys. **101**, 081715 (2007); A. V. Khaetskii, D. Loss and L. Glazman. Phys. Rev. Lett. **88**,

186802 (2002); A. Relao, J. Dukelsky and R. A. Molina, Phys. Rev. E **76**, 046223, (2007).

⁷ K. Ono *et al.*, Science **297** 1313 (2002); A. C. Johnson *et al.*, Phys. Rev. B **72** 165308 (2005).

⁸ J. Iñarrea, G. Platero and A. H. MacDonald, Phys. Rev. B **76**, 085329, (2007); J. Iñarrea, C. López-Monís, A. H. MacDonald and G. Platero, Appl. Phys. Lett., **91**, 252112 (2007); J. Iñarrea, C. López-Monís and G. Platero, Appl. Phys. Lett., **94**, 252106 (2009).

⁹ A. C. Johnson *et al.*, Nature **435**, 925 (2005).

¹⁰ A. Pfund *et al.*, Phys. Rev. Lett. **99**, 036801, (2007).

¹¹ F. H. L. Koppens *et al.*, Science **309**, 1346 (2005).

- ¹² O. N. Jouravlev and Y. Nazarov, Phys. Rev. Lett. **96**, 176804 (2006).
- ¹³ M. S. Rudner and L. S. Levitov, Phys. Rev. Lett. **99**, 036602, (2007).
- ¹⁴ R. P. Feynman, R. B. Leighton and M. Sands, *The Feynman Lecture on Physics 3*, p. 3-7, Addison-Wesley (1963).
- ¹⁵ G. Burkard, D. Loss and D. P. DiVicenzo, Phys. Rev. B **59**, 2070 (1998); R. de Sousa, X. Hu and S. Das Sarma, Phys. Rev. A **64**, 042307 (2001).
- ¹⁶ C. P. Slichter, *Principles of Magnetic Resonance*, (Springer-Verlag, Berlin, 1989).
- ¹⁷ The numbers (n, n') specify the extra number of electrons in the left and right dot respectively.
- ¹⁸ R. de Sousa, X. Hu and S. Das Sarma, Phys. Rev. Lett., **86**, 918 (2001).
- ¹⁹ S. I. Erlingsson, Y. V. Nazarov and V. Fal'ko, Phys. Rev. B, **64**, 195306 (2001).